BNL-203600-2018-TECH
C-A/AP/597

Intrinsic resonances and AC-dipole simulations of 3He in the AGS Booster

K. Hock,

September 2017

Collider Accelerator Department
Brookhaven National Laboratory

U.S. Department of Energy
USDOE Office of Science (SC), Nuclear Physics (NP) (SC-26)

DISCLAIMER

Intrinsic Resonances and AC-Dipole Simulations of ^{3}He in the AGS-Booster

Kiel Hock, François Méot, Haixin Huang, Nicholaos Tsoupas

BNL C-AD, Upton, LI, NY 11973

(Dated: September 13, 2017)

ABSTRACT

Polarized ^{3}He collisions are part of future RHIC physics programs and of the eRHIC project. The anomalous magnetic moment of ^{3}He (G=-4.184) is roughly three times greater than that of protons (G=1.793), a polarized species that is already used at the Collider-Accelerator complex at BNL. Because of the higher anomolous magnetic moment and possibly injecting into the AGS at rigidities beyond 7 T $\cdot$ m, ^{3}He may have to cross depolarizing intrinsic resonances while accelerating in the Booster. To overcome these strong intrinsic resonances we look to an AC-dipole, which will need to be installed in the Booster. An AC-dipole is a magnet that induces large betatron oscillations which forces the entire bunch to experience a stronger resonance and induce a spin flip of all particles. An artificial intrinsic resonance is created, with close proximity to the original intrinsic resonance, which requires simulations to gauge what magnet strength is required. Simulations have been performed using zgoubi regarding the resonances $0+\nu_y$, $12-\nu_y$, and $6+\nu_y$ and show that the AC-dipole is effective at overcoming these resonances. Benefits of avoiding the $0+\nu_y$ and crossing the $12-\nu_y$ and $6+\nu_y$ in the Booster presents the advantage of allowing injection above the $0+\nu_y$ in the AGS and minimizes the orbit distortions from the snakes.

CONTENTS

Abstract 1

I Introduction 3

II Spin Dynamics 3

A AC-Dipole 6

B AGS Partial Snakes 7

III Booster 8

A Booster to AGS 8

B Booster Power Supplies and Crossing Speed 9

C Booster Model 10

D AC-dipole Location 12

E Intrinsic Spin Resonances in the Booster 13

1 Fixed Energy 13

2 Froissart-Stora 13

3 Weak Resonances 14

IV AC-Dipole Spin Tracking Results 18

A AC-Dipole Setup 18

B Bunched Beam Results 19

1 0+ Crossing 20

2 12- Crossing 21

3 6+ Crossing 22

C Slow vs Fast Ramping 23

V Discussion 23

Multi-Particle Beam 24

References 26

I. INTRODUCTION

Part of the future physics programs at RHIC and eRHIC[1] are collisions with polarized ^{3}He. Due to its greater anomolous magnetic moment, polarized ^{3}He (G=-4.184) precesses faster than protons (G=1.79) which will require improvements in the synchrotrons in the RHIC accelerator chain to preserve polarization during the acceleration process, in particular the Booster. The Booster presently has no hardware for preserving spin polarization through intrinsic resonances and requires an upgrade[2].

The Booster is the first synchrotron in the RHIC accelerator chain and is the intermediary of the ion sources (be it EBIS or LINAC) and the AGS. ^{3}He will be injected into the Booster with $B\rho = 0.31\ T \cdot m$, which corresponds to $G\gamma = -4.193$, and is extracted up to $G\gamma = -10.5$ so that up to three intrinsic resonances may be encountered. A piece of hardware that occupies little space is an AC-dipole and can be used to increase intrinsic resonance strengths, so overcoming these resonances by inducing a coherent spin-flip of the particles in a bunch.

An AC-dipole is a magnet whose field oscillates at a frequency very close to the betatron frequency which results in large betatron oscillations[3]. Since the vertical polarization is to be preserved, these betatron oscillations are in the vertical plane[4], and cause the whole bunch to sample strong depolarizing horizontal fields in the quadrupoles which results in all particles to undergo a full spin flip[3, 5]. In practice, the magnet is slowly ramped up, remains at its full strength for a number of turns sufficient for spin-flipping, and is then slowly ramped down. This process of beam excitation results in minimal dilution of beam emittance[3].

An AC-dipole has been used in AGS to overcome intrinsic resonances[3] and in RHIC to manipulate the direction of spin[6]. Aside from being used to preserve polarization through intrinsic resonances, it is also used as a diagnostic tool for high precision optical measurements and has been used in this way at RHIC[7], Tevatron[8] and the LHC[9].

II. SPIN DYNAMICS

There are two types of depolarizing spin resonances encountered in a circular accelerator, intrinsic resonances and imperfection resonances. Vertical intrinsic resonances occur as the

result of vertical betatron motion and the horizontal field experienced in quadrupoles. These resonances occur when this condition is satisfied[4],

$$G\gamma = nP \pm \nu_y \tag{1}$$

In these equations, γ is the Lorentz factor, n is an integer, P is the periodicity of the accelerator, and ν_y is the vertical betatron tune. Imperfection resonances occur as a result of vertical closed orbit errors and occur when[4],

$$G\gamma = k \tag{2}$$

where k is an integer. These resonances are separated by,

$$\frac{M_o/u}{G} = 223.73 \text{ MeV/u} \tag{3}$$

where M_o is the rest mass ($M_o(^3He)$ =2808.39 MeV/c^2), which are spaced 2.34 times closer together than protons ($M_o(p)$ =938.27 MeV/c^2), which have a separation of 523.3 MeV. The anomalous magnetic moment is,

$$G = \frac{g-2}{2} \tag{4}$$

and quantifies the relativistic precession of spin in the field of synchrotron magnets; the g-factor relates the spin magnetic moment to the spin angular momentum. The term $G\gamma$ is also known as the spin tune, ν_s, and is the number of precessions the spin undergoes in one revolution around the ring.

The Froissart-Stora Formula[10],

$$\frac{P_f}{P_i} = 2\exp\Big(-\frac{\pi}{2}\frac{|\epsilon_k|^2}{\alpha}\Big) - 1 \tag{5}$$

relates the asymptotic values P_f (after) and P_i (before the resonance) of the polarization for a particle accelerated through a resonance of strength ϵ_k at a crossing speed of α. The crossing speed is defined as[4, 10],

$$\alpha = \frac{dG\gamma}{d\theta} = G\frac{1}{2\pi}\frac{\Delta E}{M_o} \tag{6}$$

ΔE is the change in energy per turn.

The Thomas-BMT equation describes the motion of the spin vector when exposed to electromagnetic field in a synchrotron and is defined as[4],

$$\frac{d\vec{S}}{dt} = \frac{e}{\gamma M_o}\vec{S} \times \Big[(1+G\gamma)\vec{B_\perp} + (1+G)\vec{B_\parallel} + (G\gamma + \frac{\gamma}{\gamma+1})\frac{\vec{E}\times\vec{\beta}}{c}\Big] \tag{7}$$

where $\vec{S}$ is the spin vector, $\vec{B}_{\perp}$ and $\vec{B}_{\parallel}$ are the transverse and longitudinal components of the magnetic field, $\vec{E}$ is the electric field and $\vec{\beta}$ is the velocity.
The resonance strength ϵ_k is the fourier amplitude of spin perturbing fields from the Thomas-BMT equation, given by[4],

$$\epsilon_k = \frac{1}{2\pi}\oint\Big[(1+G\gamma)\frac{\Delta B_{\perp}}{B\rho} + (1+G)\frac{\Delta B_{\parallel}}{B\rho}\Big]e^{iK\theta} \tag{8}$$

where θ is the azimuthal angle, K is the resonance condition. This causes ϵ_k to be non-zero only when resonant conditions are met (Eq. 1 and 2)[4].

Static depolarization[11] occurs when a spin polarization vector is allowed to oscillate freely, without being accelerated, with a close proximity Δ to the resonance, defined by[11],

$$\Delta = G\gamma - (kP - \nu_y) \tag{9}$$

The average of these oscillations at a given Δ writes,

$$\bar{S}_y^2 = \frac{1}{1+|\epsilon_k|^2/\Delta^2} \tag{10}$$

The resonance strength $|\epsilon_k|$ and the resonance proximity Δ can be solved numerically with appropriate simulation of the vertical polarization component, S_y.

For weak resonances, the motion of the spin through the resonance is well represented by a model of Fresnel integrals of the form[11],

- upstream of the resonance($\Delta < 0$),

$$\frac{p(\Delta)}{p_i} = 1 - \frac{\pi}{\alpha}|\epsilon_k|^2\Big[\Big(0.5 - C\Big(-\Delta\sqrt{\frac{\alpha}{\pi}}\Big)\Big)^2 + \Big(0.5 - S\Big(-\Delta\sqrt{\frac{\alpha}{\pi}}\Big)\Big)^2\Big] \tag{11}$$

- downstream of the resonance($\Delta > 0$),

$$\frac{p(\Delta)}{p_i} = 1 - \frac{\pi}{\alpha}|\epsilon_k|^2\Big[\Big(0.5 - C\Big(\Delta\sqrt{\frac{\alpha}{\pi}}\Big)\Big)^2 + \Big(0.5 - S\Big(\Delta\sqrt{\frac{\alpha}{\pi}}\Big)\Big)^2\Big] \tag{12}$$

where

$$C(x) = \int_0^x \cos\Big(\frac{\pi}{2}t^2\Big)dt, \qquad S(x) = \int_0^x \sin\Big(\frac{\pi}{2}t^2\Big)dt \tag{13}$$

Any of these methods (Eqs. 5, 10, 11, 12) can be used for determining resonance strength through simulation.

A. AC-Dipole

In the case of protons in the Booster, only weak imperfection resonances are crossed and polarization is preserved by inducing or correcting orbit harmonics. This technique cannot be used to overcome intrinsic resonances and only applies to imperfection resonances. Intrinsic resonances can be overcome through use of an AC-dipole. An AC-dipole is a dipole magnet designed for its field to oscillate at a frequency close to the betatron frequency. The magnet is equivalent to an inductor in a RL resonant circuit. The oscillation amplitude is ramped up as the intrinsic resonance is approached, causing the beam to oscillate at the AC dipole frequency. The beam thus samples strong horizontal fields in the quadrupoles, so increasing the resonance strength and inducing a full spin-flip.[3]

The coherent betatron amplitude is,

$$Y_{coh} = \frac{\Delta B_m l}{4\pi B\rho\delta}\beta_y \tag{14}$$

where ΔB_m is the magnetic field of the dipole, l is the length of the dipole, β_y is the vertical betatron amplitude, $\delta = \nu_{\rm y} - \nu_{\rm m}$ is the separation between the vertical betatron tune, ν_y, and the tune modulated by the AC-dipole, ν_m. The strength of the resonance created by the AC-Dipole is,

$$\epsilon_{ac} = \frac{\epsilon_k Y_{coh}}{\sigma_y} \tag{15}$$

Including the beam density distribution function, $\rho(\mathrm{y}, \mathrm{p_y})$ the Froissart-Stora formula yields[5],

$$\frac{P_f}{P_i} = \int (2e^{-\frac{\pi|\epsilon|^2}{2\alpha}} - 1)\rho(y, p_y)dydp_y \tag{16}$$

For a Gaussian beam undergoing coherent oscillations, the distribution function writes[4, 5],

$$\rho(y, p_y) = \frac{1}{2\pi\sigma_y^2}\exp\Big(-\frac{-y^2 + (p_y + \beta_{yk}\theta_k)^2}{2\sigma_y^2}\Big) \tag{17}$$

where $\beta_{\rm yk}$ is the vertical betatron amplitude at the kicker, and $\theta_{\rm k} = \Delta \mathrm{B_m l/B}\rho$ is the deflection angle from the kicker. This leads to the following[5],

$$\Big\langle\frac{\mathrm{P_f}}{\mathrm{P_i}}\Big\rangle = \frac{2}{1 + \pi|\epsilon_{\rm k}|^2/\alpha}\exp\Big(-\frac{((\beta_{\rm yk}\theta_{\rm k})^2/(2\sigma_{\rm y}^2))(\pi|\epsilon_{\rm k}|^2/\alpha)}{1 + \pi|\varepsilon|^2/\alpha}\Big) - 1 \tag{18}$$

Rearranging Eq. 18, the bunched beam requirement for a 99% spin flip can be approximated to,

$$\beta_{yk}\theta_k \geq \Big[-2\ \ln\Big(0.005\Big(1 + \frac{\pi|\epsilon_k|^2}{\alpha}\Big)\Big)\Big(1 + \frac{\alpha}{\pi|\epsilon_k|^2}\Big)\Big]^{1/2}\sigma_y \tag{19}$$

which is sufficient for a single, well-isolated, resonance. Due to the artificial resonance created at δ away from the intrinsic resonance, simulations are required to get the magnet strength for a spin-flip.

B. AGS Partial Snakes

To avoid imperfection resonances, and vertical intrinsic resonances in the AGS, there are two partial helical dipoles in place, a superconducting one, "cold snake," and a normal conducting one, "warm snake." Unlike a full snake which causes a full spin-flip each time a particle passes through, partial snakes rotate the spin by an angle $\chi < 180^o$. Because of this additional rotation with each turn, ν_s is no longer linearly dependent on $G\gamma$ and instead has the form[12],

$$\nu_s = \frac{1}{\pi}\arccos(\cos\frac{\chi_c}{2}\cos\frac{\chi_w}{2}\cos[G\gamma\pi] - \sin\frac{\chi_c}{2}\sin\frac{\chi_w}{2}\cos[G\gamma\frac{\pi}{3}]) \tag{20}$$

where χ_c and χ_w are the rotation angle from the cold and warm partial snakes, the π and $\pi/3$ terms result from the relative location of the two snakes in the ring which is 1/3 of the ring apart, the results of which are shown in Fig. 1. Because with each pass there is only a partial rotation of the spin vector, the stable spin direction also has a dependence on $G\gamma$ and the rotation angle from each snake. The vertical component of the stable spin direction writes[12],

$$\cos\alpha_3 = \frac{1}{\sin\ \pi\nu_s}\arccos(cos\frac{\chi_c}{2}\cos\frac{\chi_w}{2}\cos[G\gamma\pi] - \sin\frac{\chi_c}{2}\sin\frac{\chi_w}{2}\cos[G\gamma\frac{\pi}{3}]) \tag{21}$$

where α_3 is the angle between the spin vector and the vertical axis. This shows that the stable spin direction is closest to vertical every $G\gamma = 3n + 1.5$, where n is an integer. This is important to consider when devising an extraction/injection scheme from Booster into AGS, accounting for spin matching. Results of Eq. 20 and 21 are shown in Fig. 1 for a range of Gγ values.

On the other hand, the snakes also cause substantial optics perturbations at injection rigidity of Bρ = 7 T $\cdot$ m. These perturbations include beta function modulation, vertical dispersion, and coupling[13]. For this reason ^{3}He injection at higher rigidity, up to $G\gamma$=-10.5 ($B\rho$=10.8) is investigated, and as part of that, possible spin resonances crossing in Booster are discussed.

III. BOOSTER

A. Booster to AGS

When concerned about preserving the polarization, there are several options for designing a booster magnet cycle. As seen earlier, spin matching imposes extraction from the Booster at either $G\gamma = -7.5$ or $G\gamma = -10.5$. Acceleration to $G\gamma = -7.5$ is simple if $\nu_y < 4.1$ at injection, the 0+ resonance is avoided because $G\gamma_{injection} = -4.19$, and if $\nu_y < 4.5$ at extraction $G\gamma = -7.5$, the 12- resonance is also avoided. However, it is preferable to extract at $G\gamma = -10.5$ as higher rigidity causes the optics distortions from the cold snake in the AGS to be minimized[13]. In this case the vertical tune ν_y could be maintained below 4.1 to avoid the 0+ resonance and pass through 12- and 6+ resonances. This is shown as an example in Fig. 2 where a particle is tracked from $G\gamma$=-4.19 to $G\gamma$=-10.5 with ν_y=4.1.

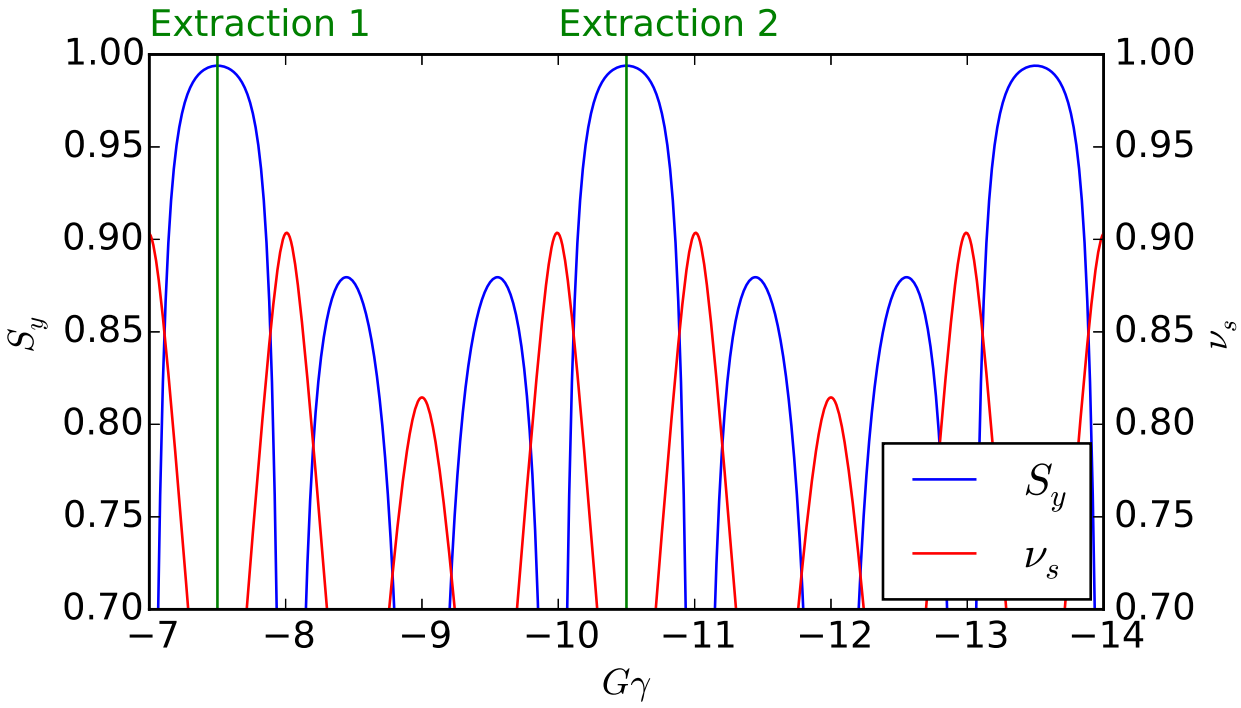

FIG. 1: Spin tune, ν_s (Eq. 20), and the vertical component (Eq. 21) of the stable spin direction in the AGS, S_y. The two possible extractions at $G\gamma$=-7.5 and $G\gamma$=-10.5 correspond to a stable spin direction closest to the vertical.

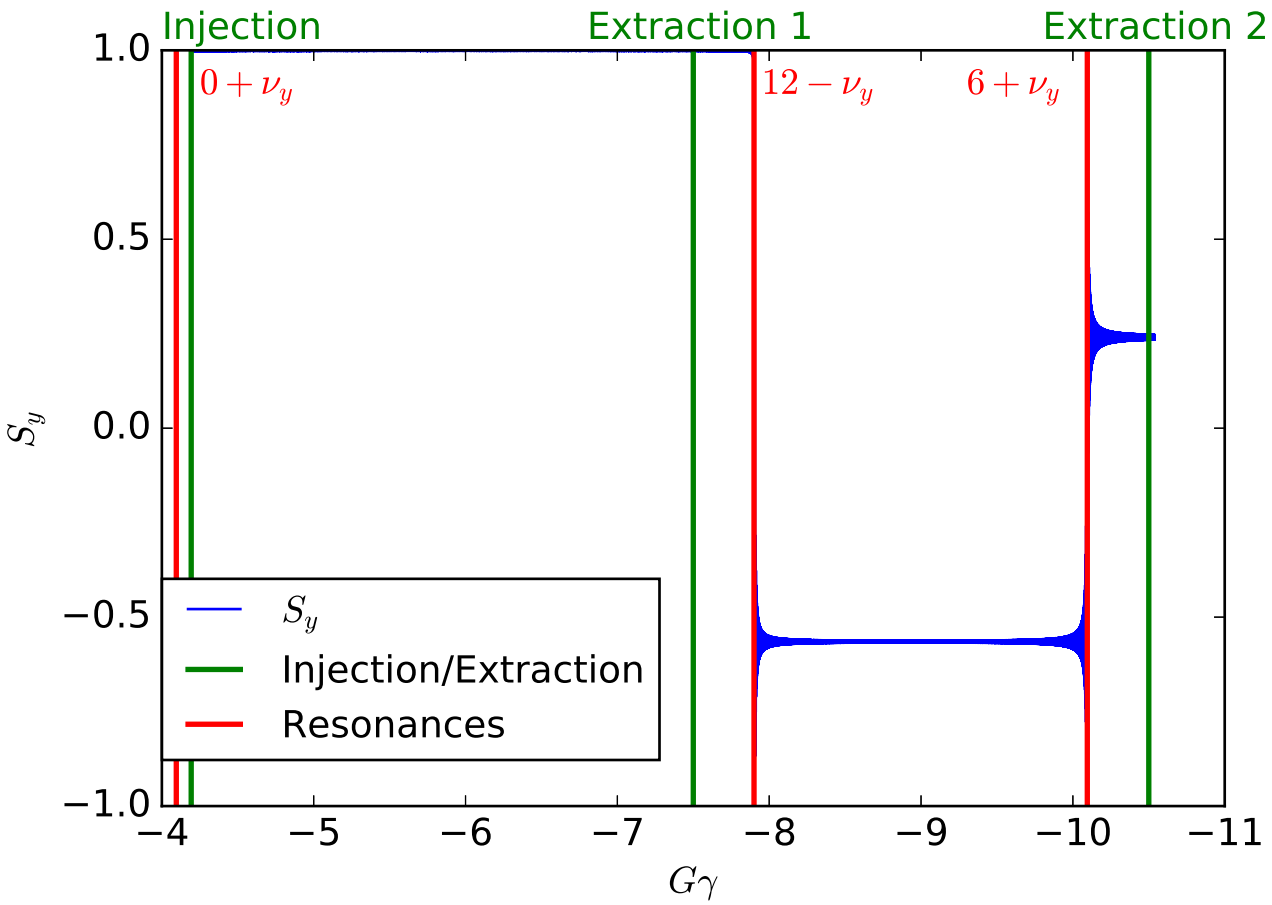

FIG. 2: A particle (blue) is tracked from injection, $G\gamma$=-4.19, to $G\gamma$=-10.5, with ν_y=4.1. Intrinsic resonances (red), injection and extraction $G\gamma$ values (green) are marked.

B. Booster Power Supplies and Crossing Speed

Saturation effects in the Booster quadrupoles are observable at $G\gamma = -10.5$, which limits the range of tunes that we can use[14]. There are six transformers for the Booster Main Magnet, four of which are limited to 3000A or Bρ = 9.5 T$\cdot$m which would require exceeding this limit by 13.5% to reach $G\gamma = -10.5$ (Bρ = 10.8 T $\cdot$ m). Two of these transformers are able to reach 5000A, which would result in a slower ramp rate (a third the ramp rate compared to having all six transformer modules). These two different ramp rates correspond to a crossing speed (Eq. 6) of $\alpha = 7.9611\times^{-6}$ (fast) and $\alpha = 2.6537\times^{-6}$ (slow) respectively.

TABLE I: Relevant beam parameters at important stages of the booster cycle. ε_{rms} is extrapolated from $\varepsilon_{\mathrm{N}} = 5\ \pi$ mm mrad.

Parameter	Injection	$0 + \lvert\nu_z\rvert$	$12 - \lvert\nu_z\rvert$	$6 + \lvert\nu_z\rvert$	Extraction 1	Extraction 2	Units
$G\gamma$	-4.19312	-4.7	-7.8	-10.3	-7.5	-10.5	-
ν_z	< 4.1	4.7	4.2	4.4	-	-	-
$B\rho$	0.307	2.37	7.36	10.60	6.95	10.78	$\mathrm{T} \cdot \mathrm{m}$
f_{rev}	0.097	0.674	1.254	1.357	1.236	1.364	MHz
ε_{rms}	-	1.60	0.54	0.37	0.56	0.36	π mm mrad

C. Booster Model

Simulations are done using a python interface for zgoubi, known as pyzgoubi[15, 16] which provides a MADx-like syntax for elements, access to all python modules, and the zgoubi engine that handles all the tracking. The lattice results from the zgoubi model agree closely with those from MADx (which has been shown to accurately represent the Booster[17]), shown in Table II and Fig. 3. Although Table II shows a close agreement between the zgoubi and MADx model, the absolute bare tune difference over the range of $B\rho$ the Main Magnet is able to produce (up to 5000A) is $|\nu_{MADx} - \nu_{zgoubi}| < 0.0005$.

TABLE II: Comparison of MADx and zgoubi model results given for optics at $G\gamma = 12 - \nu_y$.

	MADx	zgoubi	Units
Orbit Length	201.7800	201.7799	m
$\nu_{\mathrm{x}},\ \nu_{\mathrm{y}}$	4.5000, 4.1953	4.5000, 4.1953	-
$\xi_{\mathrm{x}},\ \xi_{\mathrm{y}}$	-8.0496, -1.1511	-7.2790, -1.1546	-
$\beta_{\mathrm{max}},\ \beta_{\mathrm{min}}$	13.6125, 4.7690	13.6126, 4.7699	m

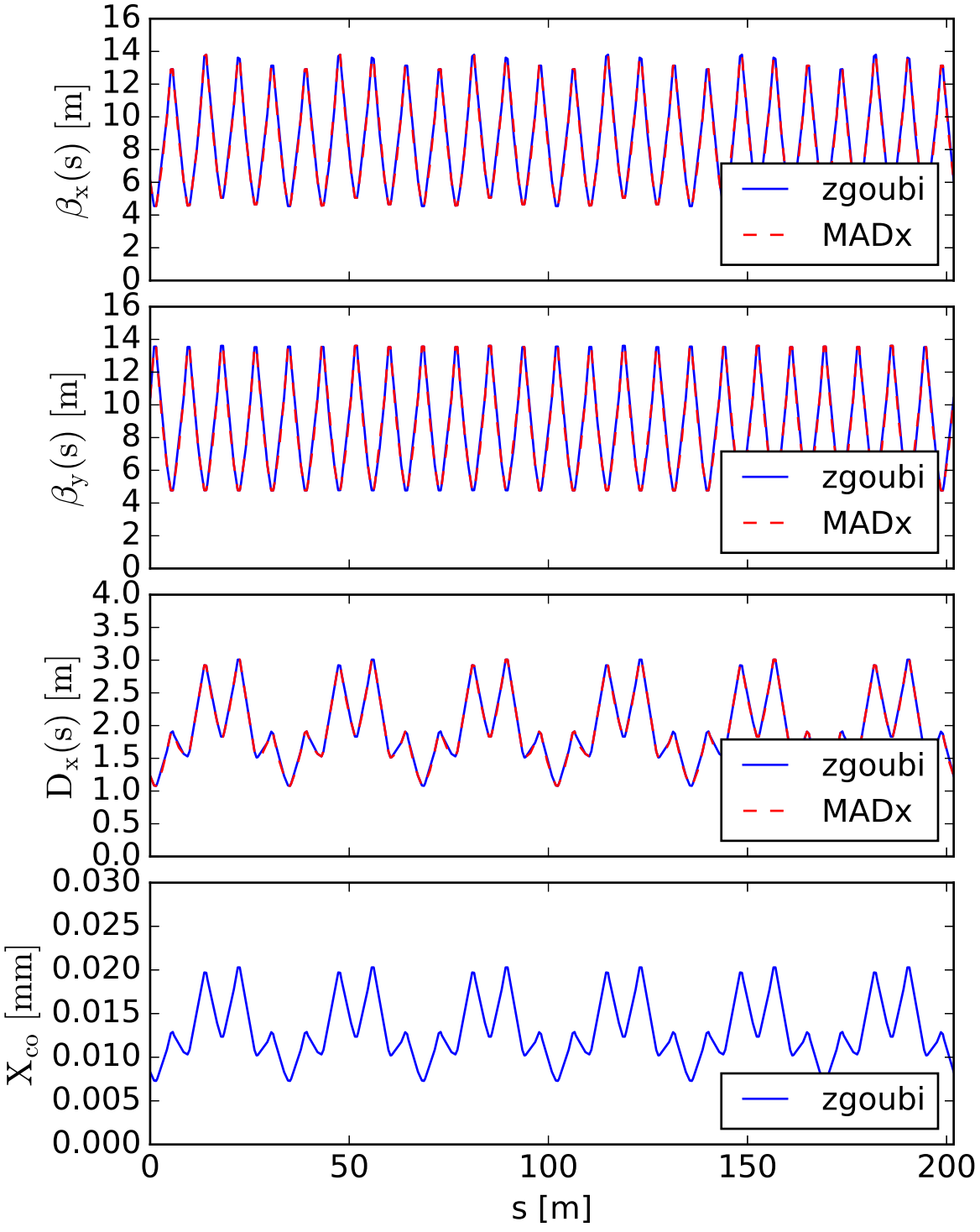

FIG. 3: Horizontal and vertical beta functions, and dispersion functions, from zgoubi (blue) and MADx (green). There is also a small non-zero closed orbit in zgoubi which does not affect the results.

D. AC-dipole Location

The booster has 36 dipole magnets, with a curvature radius ρ=13.866m, and 48 quadrupoles broken up into 6 superperiods. Each superperiod, labeled A through F, contains eight half-cells numbered 1 through 8 where every 3$^{\text{rd}}$ and 6$^{\text{th}}$ half-cells has a drift section in place of a main sector dipole. Of these 12 significant drifts in the accelerator, the majority of them are occupied by RF cavities (A3, A6, B3, E6), injection and extraction devices (C3 inflector for ion injection, D3 and D6 septa for slow extracted beam, F3 and F6 septa for fast extracted beam), instrumentation (Wall current monitors, Ionization profile monitors, Tune kickers, etc.). This leaves E3, where the present tune kicker exists, to locate the AC-dipole.

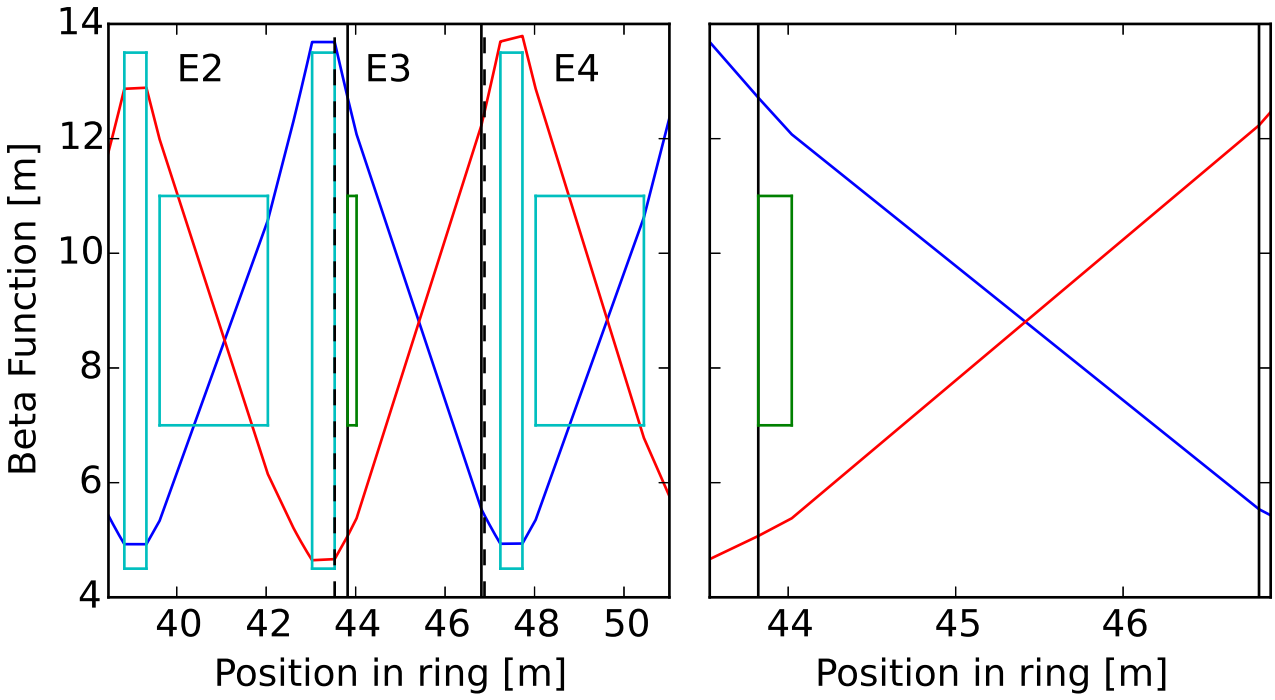

(a) (b)

FIG. 4: (a) A snapshot of sections E2 through E4. Dipoles are short rectangles, Quadrupoles are tall rectangles, vertical betatron function in blue, horizontal betatron functions in red, AC-dipole at E3 (l_{AC}=0.20 m) in green. Space between dotted black lines is available, space between solid black lines show the available space consistent with the spacing else where in the accelerator. (b) This is a zoomed in area of the space between the dotted lines in Fig 4a, including the AC-dipole as used in the simulations.

Since the amplitude of the vertical coherent betatron oscillation varies in proportion with the vertical beta function at the kicker (Eq. 14), it is important to have the AC-dipole placed where the beta function is close to maximum. For the purpose of these simulations, a length of 20 cm is used for the AC-dipole which is placed close to the nearest vertically focusing quadrupole in section E3, Fig. 4a (the present location of the tune kicker). Fig. 4b shows a close up of the area in E3 between the nearest optical elements. Results are given in Table III for the three resonances covered (0+, 12-, 6+).

E. Intrinsic Spin Resonances in the Booster

For the sake of benchmarking and understanding, three different methods are implemented with zgoubi and used to calculate the strength of the intrinsic depolarizing resonances. The results are also compared to results from DEPOL[18] using optics provided by MADx outputs, and summarized in Table III for the 0+, 12-, and 6+ resonances.

1. Fixed Energy

One way to calculate the strength of the resonances is the static depolarization method, Eq. 10. Tracking is performed for a few hundred turns without acceleration, some distance $\Delta = \mathrm{G}\gamma - (\mathrm{kP} \pm \nu_\mathrm{y})$ from the resonance. This tracking is iterated for a few values of Δ. The ensemble is then fitted using Eq. 10, so yielding ϵ_k and the exact tune value at the resonance.

2. Froissart-Stora

Finding the resonance strength through Froissart-Stora requires a particle to be accelerated through the resonance, Eq. 5. The asymptotic value of the final polarization is calculated by taking an average of the vertical spin component for the last 1,000 turns of the tracking, and is compared to its initial value by means of Eq. 5.

3. Weak Resonances

For weak resonances, a small emittance particle is accelerated through the resonance so the Fresnel-integral can be implemented. Eq. 11 and Eq. 12 are used to fit the vertical spin motion, before and after the resonance, which yields the resonance strength, ϵ_k, and the location of the resonance, Δ.

TABLE III: Summary of resonant $G\gamma$ values and resonance strengths in the booster, using three different methods discussed in addition to results from DEPOL.

		Static		Froissart-Stora		Fresnel-Integral		DEPOL
Resonance	$\varepsilon_{rms}(\mu m)$	$\lvert\epsilon_k\rvert$	$\lvert G\gamma_R\rvert$	$\lvert\epsilon_k\rvert$	P_f	$\lvert\epsilon_k\rvert$	$\lvert G\gamma_R\rvert$	ϵ_k
0+	0.001	0.000107	4.6953	0.000107	0.987	0.000107	4.6954	0.000109
	0.1	0.001066	4.6953	0.001074	0.010			0.001090
	1.60	0.004330	4.6953					0.004359
	10	0.010714	4.6953					0.010899
12-	0.001	0.000126	7.8047	0.000126	0.981	0.000126	7.8049	0.000125
	0.1	0.001256	7.8047	0.001258	-0.216			0.001246
	0.525	0.002914	7.8047					0.002855
	10	0.012669	7.8047					0.012460
6+	0.0001	0.000072	10.3953	0.000077	0.993	0.000078	10.3953	0.000074
	0.001	0.000234	10.3953	0.000245	0.930			0.000233
	0.1	0.002342	10.3953	0.002329	-0.919			0.002327
	0.369	0.004513	10.3953					0.004469
	10	0.023611	10.3953					0.023265

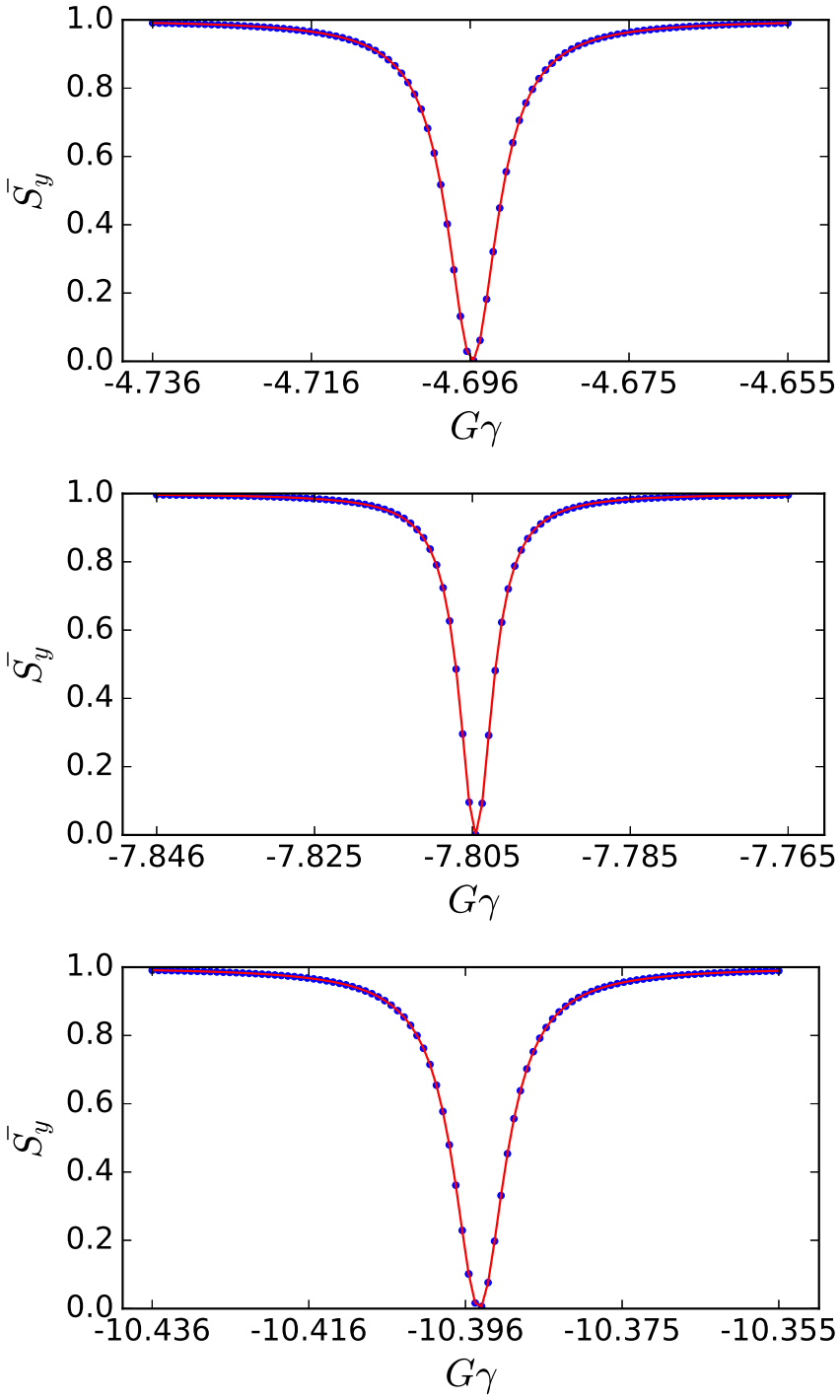

FIG. 5: A simulation of the component of the stable spin direction in the vicinity of the three resonances (0+ (top), 12- (center), 6+ (bottom)) using the static depolarization method showing data points (blue) and the fit results using Eq. 10 (red). (top) 0+ resonance shown with a $\varepsilon_{\rm y} = 1.60$ μm particle yields $|G\gamma_R|$=4.6953 and $|\epsilon_k|$=0.004330. (center) 12- resonance shown with a $\varepsilon_{\rm y} = 0.53$ μm particle yields $|G\gamma_R|$=7.8047 and $|\epsilon_k|$=0.002914. (bottom) 6+ resonance shown with a $\varepsilon_{\rm y} = 0.37$ μm particle yields $|G\gamma_R|$=10.3953 and $|\epsilon_k|$=0.004513.

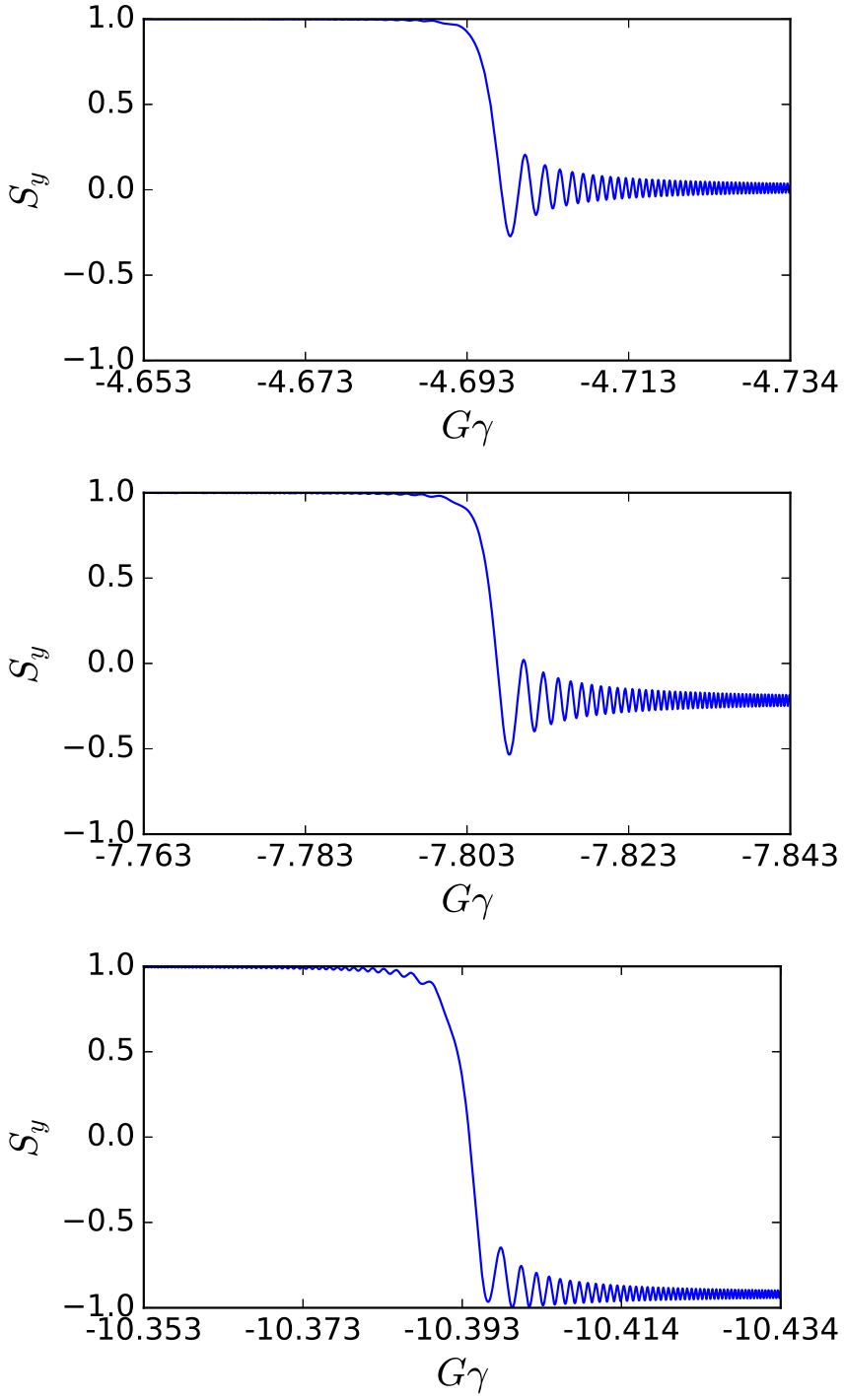

FIG. 6: Computations of the resonance strengths using the Froissart-Stora Formula for 0+, 12-, 6+ resonance with a $\varepsilon_{\rm y} = 0.1$ μm invariant particle. (top) 0+ resonance yields P_f=1.0% and $|\epsilon_k|$=0.001074. (center) 12- resonance yields P_f=-21.6% and $|\epsilon_k|$=0.001258. (bottom) 6+ resonance yields P_f=-91.9% and $|\epsilon_k|$=0.002329.

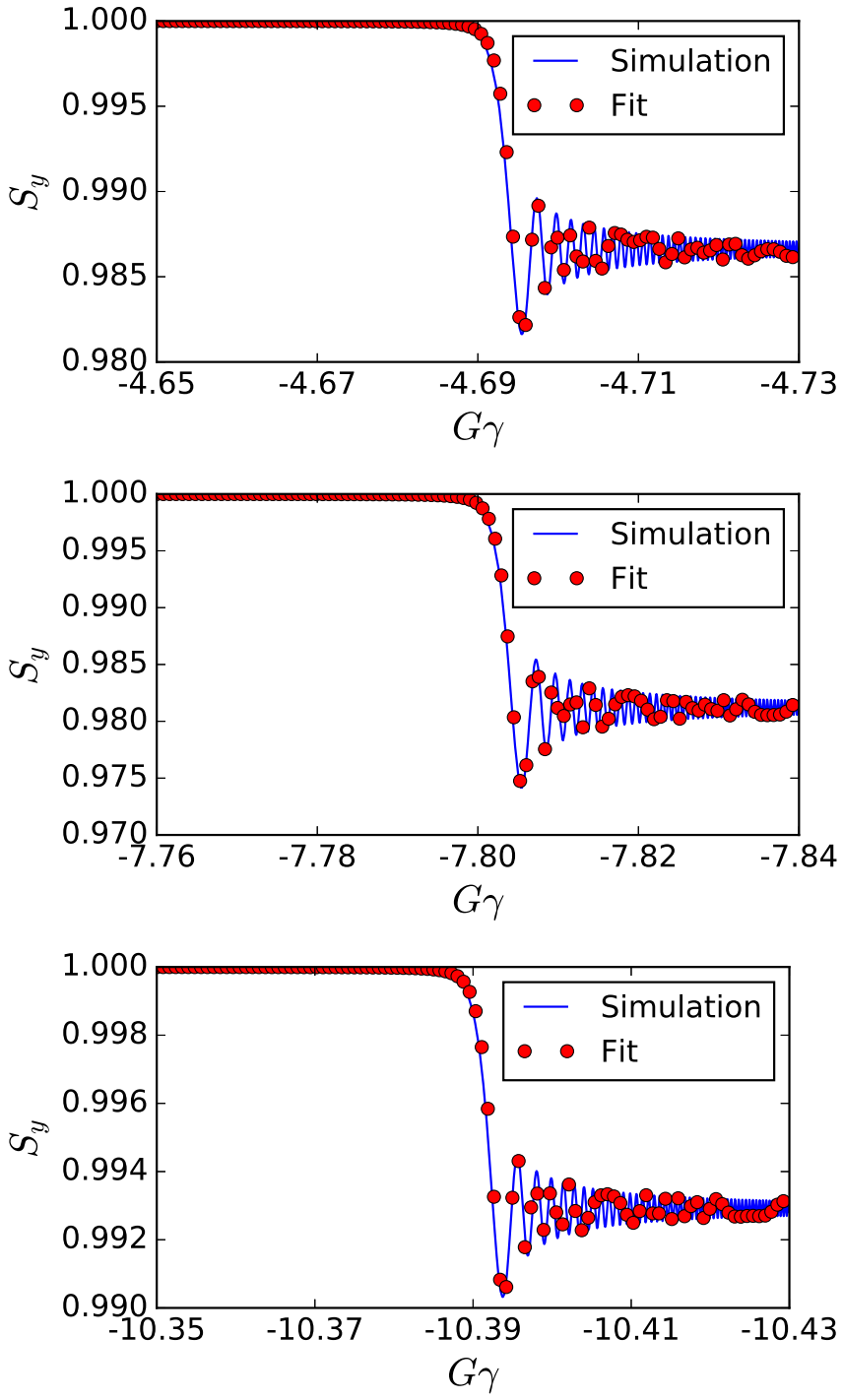

FIG. 7: Simulation of spin motion in the vertical direction of a particle as it transits the three resonances (0+ (top), 12- (center), 6+ (bottom)) with data points (blue) and the fit results using Eqs. 11 and 12 (red). (top) 0+ resonance shown with a $\varepsilon_{\rm y} = 0.001$ μm particle, $|G\gamma_R|$=4.6954, $|\epsilon_k|$=0.00106604. (center) 12- resonance shown with a $\varepsilon_{\rm y} = 0.001$ μm particle, $|G\gamma_R|$=7.8049, $|\epsilon_k|$=0.00012575. (bottom) 6+ resonance shown with a $\varepsilon_{\rm y} = 0.0001$ μm particle, $|G\gamma_R|$=10.3953, $|\epsilon_k|$=0.00007754.

IV. AC-DIPOLE SPIN TRACKING RESULTS

A. AC-Dipole Setup

The duration of the AC-dipole cycle is determined by the strength of the resonance and the length of the ramp period. The duration of the ramp to get to the magnet's full strength, N_{up}, is determined so it satisfies the adiabaticity condition[19], and is set so that $N_{up} > T_s$, where T_s is the synchrotron period. The ramp begins at $G\gamma_o = G\gamma_R - 7\epsilon_k$[20], where γ_o is the value at the start of the ramp and γ_R corresponds to where the resonance occurs. Fig. 8a shows an AC-Dipole cycle used for the simulations of a cycle with 6000 turns up, 5000 turns flat, and 6000 turns to ramp down. Fig. 8b shows the center of bunch motion while the dipole is at its full strength. As a reference, the 95% normalized emittance of the ^{3}He beam ($\varepsilon_{N,95\%}$) observed in Run 14 was 4.78 π mm mrad at AGS injection ($G\gamma = -7.817$)[21], thus a 95% normalized emittance of 5.0 π mm mrad is used for these simulations.

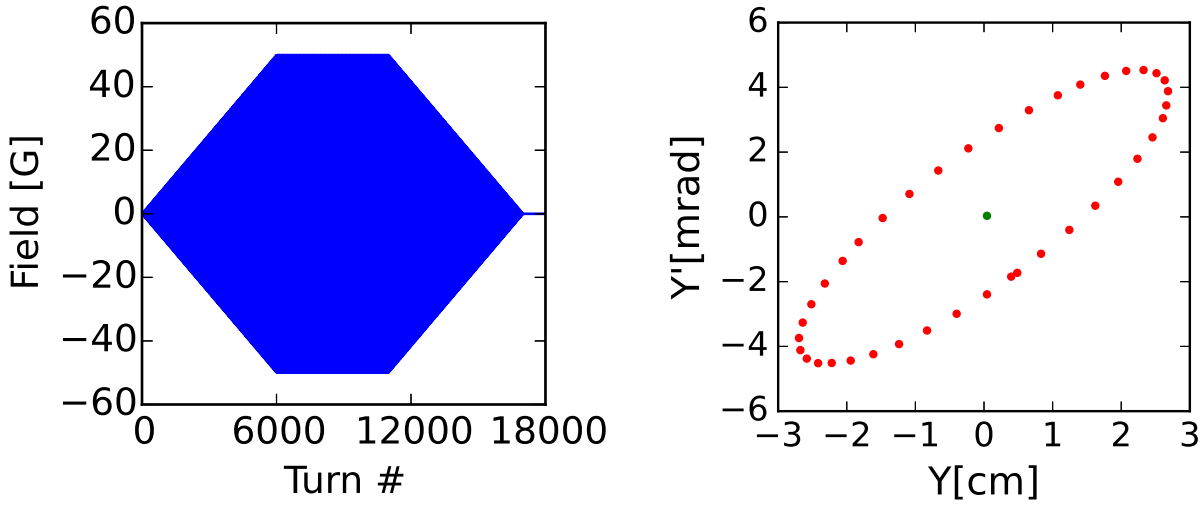

(a) (b)

FIG. 8: (a) An example AC-dipole cycle plotting the (densely) oscillating magnetic field with number of turns, $N_{up} = 6000$, $N_{flat} = 5000$, $N_{down} = 6000$, $\nu_m = 0.21$. (b) Center of mass for the initial distribution of particles (green), prior to the AC-dipole starting to ramp; center of mass of the whole bunch at maximum AC-dipole strength for 50 turns (red).

B. Bunched Beam Results

A many particle bunch with a Gaussian distribution is generated in the vertical plane with a Gaussian momentum distribution, respectively $\varepsilon_{\mathrm{N},95\%} = 5\ \pi$ mm mrad and $\sigma_P = 0.001/\xi_y$, where ξ_y is the vertical chromaticity, so that the one sigma particle will have a tune shift of $\pm$ 0.001 from the synchronous particle. Table IV summarizes the AC-dipole requirements for the 0+, 12-, and 6+ intrinsic resonances. Motion of the stable spin direction across the resonance, vertical bunch motion during the AC-dipole ramp, and initial and final vertical beam distributions are shown in Figures 9 (0+), 10 (12-), 11 (6+). For situations where there is a significant dilution of the emittance, the ramp of the AC-dipole is made more adiabatic (ramp up to full strength is longer). To estimate the emittance growth, a fit is done on the distribution at the start and end of the cycle. These widths are converted to ε_N and compared to each other by $\varepsilon_{\mathrm{r}} = \varepsilon_{\mathrm{N,final}}/\varepsilon_{\mathrm{N},0}$ to gauge if there is any growth. For each of these instances the emittance growth is minimial except for the 0+ crossing with a non-zero momentum spread which experienced a 20% increase.

TABLE IV: Summary of AC-dipole parameters at each resonance to achieve a -99% spin-flip. There are two columns for each resonance, one that corresponds to zero momentum spread,$\Delta\nu_y$ =0.0, and the second that corresponds to a momentum spread so the one-sigma particle has a tune shift, $\Delta\nu_y = \nu_y - \nu_y(\sigma_p)$, of 0.001.

Parameter	$G\gamma = 0+$		$G\gamma = 12-$		$G\gamma = 6+$	
$\lvert G\gamma\rvert$	4.7		7.8		10.4	
$\Delta\nu_y$	0	0.001	0	0.001	0	0.001
$B_m l$	8.71	11.96	14.83	21.40	16.52	23.26
$B_m l(theory)$	6.83	-	10.74	-	14.56	-
$\langle P_f \rangle$	-99.0	-99.0	-99.0	-99.0	-99.0	-99.0
ε_r	1.00	1.21	1.03	1.06	1.04	1.04

1. 0+ Crossing

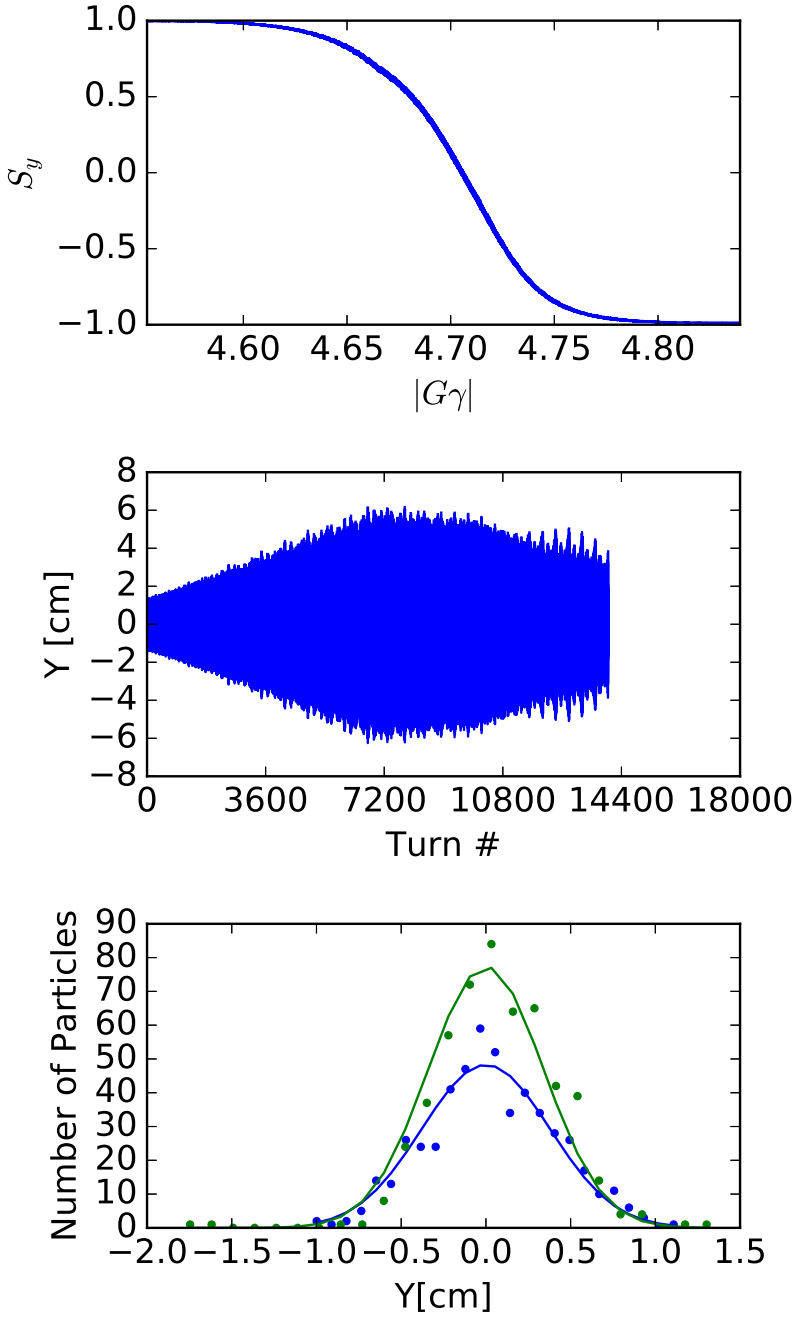

FIG. 9: $G\gamma = 0+, \nu_y = 4.695, \nu_m = \nu_y + 0.010$, $\Delta \mathrm{B_m l} = 8.71$ G · m, $P_f = -99.0\%$, $\varepsilon_r = 1.20$. (top) The component of the spin vector in the vertical plane as the resonance is crossed with the AC-dipole on. (center) Amplitude of the vertical bunch motion during the AC-dipole ramp. (bottom) Final bunch distribution (green) and initial distribution (blue) used to calculate the change in normalized emittance.

2. 12- Crossing

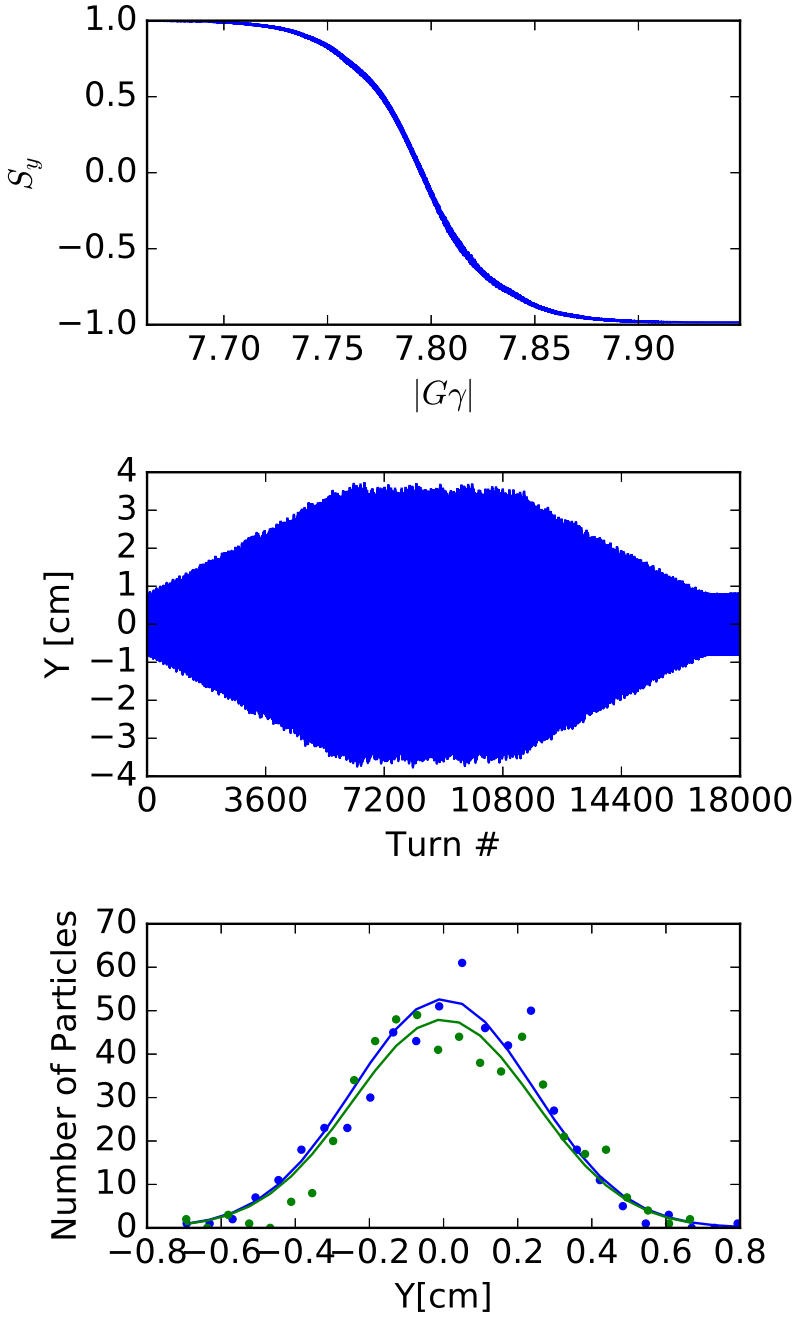

FIG. 10: $G\gamma = 12-, \nu_y = 4.195, \nu_m = \nu_y + 0.010$, $\Delta \mathrm{B_m l} = 13.27\ \mathrm{G \cdot m}$, $P_f = -99.\%,\ \varepsilon_r = 1.04$. (top) The component of the spin vector in the vertical plane as the resonance is crossed with the AC-dipole on. (center) Amplitude of the vertical bunch motion during the AC-dipole ramp. (bottom) Final bunch distribution (green) and initial distribution (blue) used to calculate the change in normalized emittance.

3. 6+ Crossing

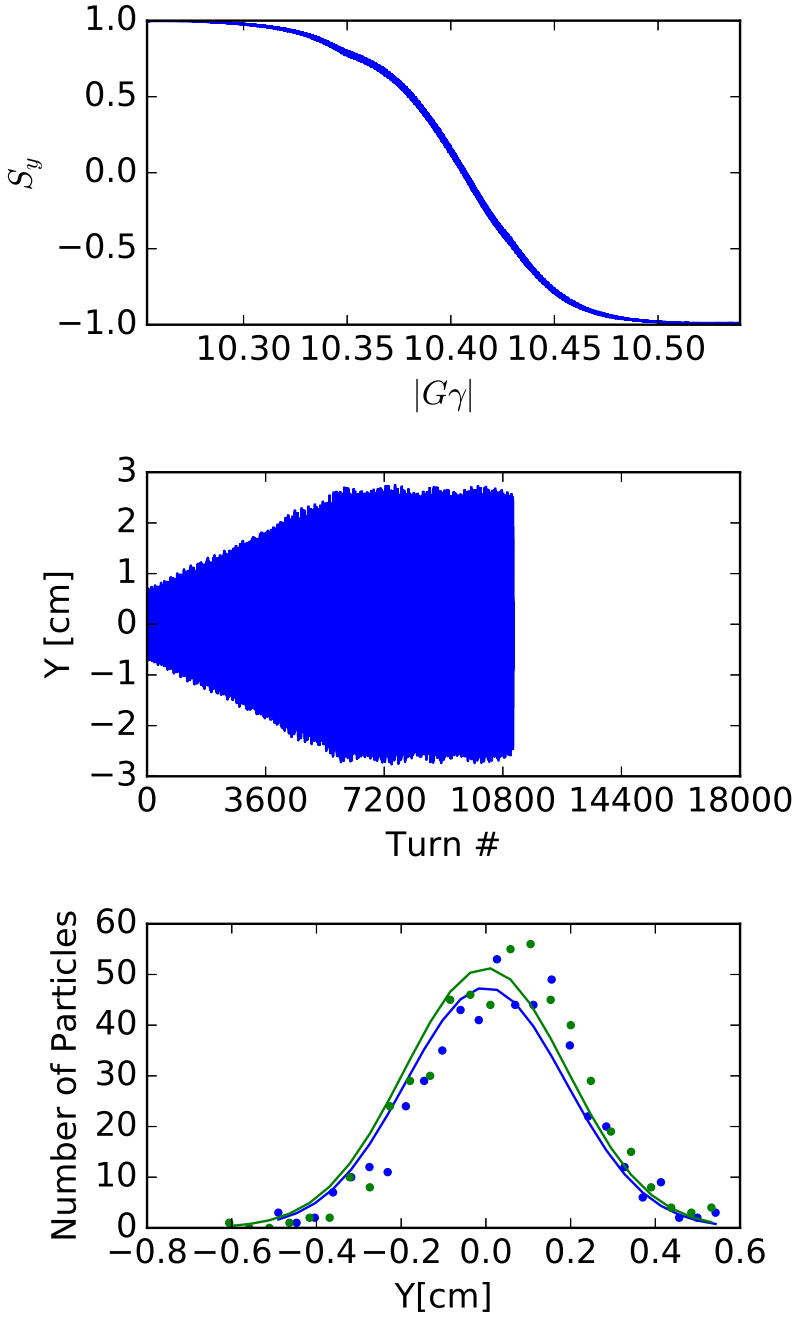

FIG. 11: $G\gamma = 6+, \nu_y = 4.395, \nu_m = \nu_y + 0.010$, $\Delta \mathrm{B_m l} = 14.78$ G · m, $P_f = -99.0\%$, $\varepsilon_r = 1.04$. (top) The component of the spin vector in the vertical plane as the resonance is crossed with the AC-dipole on. (center) Amplitude of the vertical bunch motion during the AC-dipole ramp. (bottom) Final bunch distribution (green) and initial distribution (blue) used to calculate the change in normalized emittance.

C. Slow vs Fast Ramping

The difference between the slow and fast ramping are minimal when considering the effectiveness of an AC-dipole, where the crossing speed is three times faster for the case of the fast ramp. From Eq. 19, with the difference in crossing speeds, AC-dipole requirements for crossing 12- are 10.74 G · m for slow and 9.35 G · m for fast (a 15 % difference), for a $\varepsilon_{\mathrm{N}} = 5\pi$ mm mrad bunch. The results from spin tracking, with the momentum spread discussed earlier, show that the requirements are 21.4 G · m for the slow ramp and 18.0 G · m for the fast ramp (a 19% difference).

V. DISCUSSION

Simulations show that the AC dipole is effective at overcoming intrinsic spin resonances in the Booster. It allows this by inducing a spin flip through the 0+, 12- and 6+ resonance. A slight dilution of the vertical emittance is observed for the 0+, however that resonance may be avoided. Increasing the number of particles used in bunched beam simulations would improve the error associated with the estimated emittance growth and AC-Dipole performance. Any improvements on emittance will improve AC-dipole performance. The difference in AC-dipole requirements for the fast and slow ramp is relatively small ($\sim 15\%$).

Several aspects of machine requirements for the AC-dipole will be addressed in a future document. These include: whether there is sufficient vertical aperture in the dipole beampipe to accept these large betatron oscillations; how the rapid change in f_{rev} would affect the reliability of the AC-dipole, effects of implementing use of sextupoles while the AC-dipole is on; effectiveness of spin-flip with a more realistic momentum spread; as well as simulations with protons crossing the 0+ resonance. Protons crossing the 0+ resonance has machine parameters similar to that of ^{3}He crossing the 12- resonance and provides a convenient proof-of-principle during the interim of the polarized ^{3}He source construction.

MULTI-PARTICLE BEAM

A brute force program was written to simulate the performance of the AC-dipole for multiple machine configurations. This program was made to utilize multiple CPUs to reduce computing time. That is, each configuration would get its own CPU core with multiple configurations running simultaneously. Machine configurations consisted of: $10G \leq \Delta B_m \leq 100G$ in increments of 10G, $\nu_m = \nu_z + \delta\nu$ with $-0.015 \leq \delta\nu \leq 0.015$. For each configuration, the final polarization and the emittance are analyzed and reported. The bunch that is tracked has 9 particles with the following configuration:

ϵ_{RMS} = 0, 5, 10 π mm mrad

$\delta\nu_z$ = -0.002, 0.0, +0.002

Fig. 12 justifies using $\delta\nu$ of 0.01 since the emittance is recoverable. Fig. 13 is an example of other data that can be extracted from this exercise; the final polarization and emittance at various strengths.

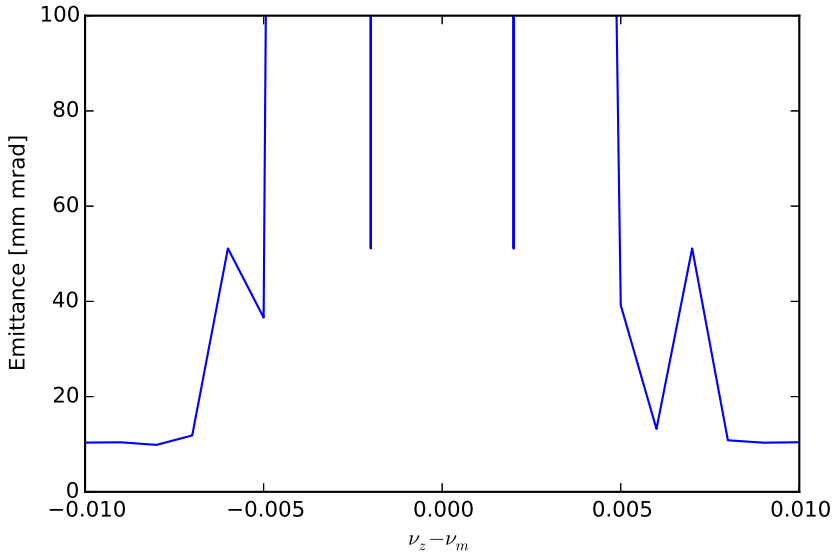

FIG. 12: $G\gamma = 12-,\ B_m = 70.0G,\ \nu_z = 4.695,\ \varepsilon = 10\pi$

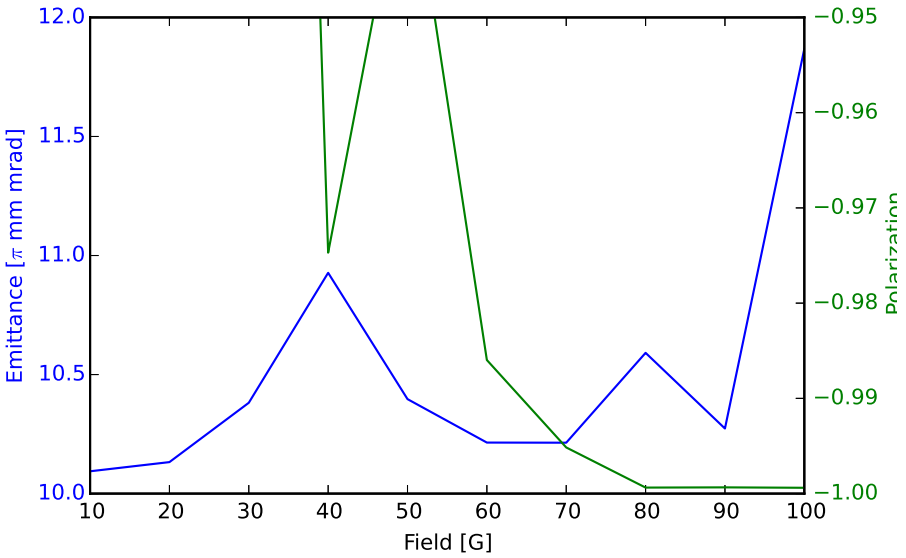

FIG. 13: $G\gamma = 6+$

[1] E. Aschenauer et al., "Opportunities for Polarized He-3 in RHIC and EIC," in *Proceedings of RIKEN BNL Research Center Workshop*, 2011.

[2] H. Huang et al, "Optics Setup in the AGS and AGS Booster for Polarized Helion Beam," in *IPAC Proceedings*, 2014.

[3] M. Bai, *Overcoming the Intrinsic Spin Resonance by Using an RF Dipole*. PhD thesis, Indiana University, 1999.

[4] S. Y. Lee, *Spin Dynamics and Snakes in Synchrotrons*. World Scientific, 1997.

[5] M. Bai et al., "Overcoming the Intrinsic Spin Resonance using Resonance Island created by RF Dipole," tech. rep., C-AD Tech Note, 1997.

[6] M. Bai et al., "RHIC Spin Flipper Commisioning Results," in *IPAC Proceedings*, 2012.

[7] X. Shen et al., "AC Dipole Based Optics Measurement and Correction at RHIC," in *PAC Proceedings*, 2013.

[8] R. Miyamoto et al., "Nonlinear Dynamics Studies in the Fermilab Tevatron Using an AC Dipole," in *PAC Proceedings*, 2009.

[9] R. Tomás et al., "Reliable Operation of the AC Dipole in the LHC," in *EPAC Proceedings*, 2008.

[10] M. Froissart, R. Stora, "Depolarisation d'un faisceau de protons polarises dans un synchrotron," *Nuclear Instruments and Methods*, vol. 7:297-305, 1959.

[11] F. Méot, "Spin Tracking simulations in AGS based on ray-tracing methods - bare lattice, no snakes," tech. rep., C-AD Tech Note, 2009.

[12] F. Lin, *Towards Full Preservation of Polarization of Proton Beams in AGS*. PhD thesis, Indiana University, December 2007.

[13] A. Luccio et al., "Cold AGS Snake Optimization by Modeling," tech. rep., C-AD Tech Note, 2003.

[14] E. Bleser, "Booster Short Quadrupole Measurements," tech. rep., C-AD Tech Note, 1990.

[15] F. Méot, *Zgoubi User's Guide*. https://sourceforge.net/projects/zgoubi/?source=directory, 2017.

[16] S. Tygier et al., "The PyZgoubi Framework and the Simulation of Dynamic Aperture in Fixed-Field Alternating Gradient Accelerators," *Nuclear Instruments and Methods in Physics*,

vol. 775, pp. 15–26, 2015.

[17] K. Brown et al., "A high precision model of Booster Tune Control," tech. rep., C-AD Tech Note, 2002.

[18] E. Courant et al., "The Accleration of Polarized Protons in Circular Accelerators," tech. rep., C-AD Tech Note, 1980.

[19] S. Y. Lee, *Accelerator Physics*. World Scientific, 2012.

[20] The $7|\varepsilon_k|$ arises from solving Eq. 10, $\Delta = \sqrt{\frac{S_y^2}{S_y^2-1}}\epsilon_k$, for $S_y = 99\%$.[11].

[21] K. Gardner, "Injector Setup for Helions in RHIC," 2015. BNL C-AD Spin Meeting.